IOP Conf. Series: Journal of Physics: Conf. Series **1293** (2019) 012027 doi:10.1088/1742-6596/1293/1/012027

Antiferromagnetism, superconductivity and phase diagram in the three-band model of high-temperature cuprates

Takashi Yanagisawa

Electronics and Photonics Research Institute, National Institute of Advanced Industrial Science and Technology (AIST), Tsukuba Central 2, 1-1-1 Umezono, Tsukuba 305-8568, Japan

E-mail: t-yanagisawa@aist.go.jp

Abstract. We investigate the ground state of the two-dimensional three-band d-p model for for high-temperature superconductors on the basis of a variational Monte Carlo method. We employ an optimization variational Monte Carlo method that we have developed recently. The many-body wave function is improved beyond the Gutzwiller ansatz by adopting the wave function in the form $\psi = \exp(-S)\psi_G$ where ψ_G represents the Gutzwiller function and S is a kinetic operator. The strong magnetic correlation and also superconductivity (SC) are induced by the on-site Coulomb repulsive interaction. It is important to clarify the phase diagram that includes superconductive phase and antiferromagnetic phase. We show the phase diagram to show the antiferromagnetic region in the parameter space. High-temperature superconductivity may occur in the strongly correlated region near the antiferromagnetic boundary.

1. Introduction

The physics of high-temperature superconductivity has been studied intensively for about 30 years since the discovery of cuprate high-temperature superconductors[1]. It has been established that the Cooper pairs of cuprate superconductors have the d-wave symmetry. This indicates that the electron correlation plays an important role for the appearance of high-temperature superconductivity. It is also known that cuprate parent materials without carries are Mott insulators.

The CuO_2 plane is commonly contained in high-temperature cuprates. The CuO_2 plane consists of oxygen atoms and copper atoms and the electronic model for this plane is the model with d and p orbitals called the d-p model (or three-band Hubbard model)[2, 3, 4, 5, 6, 7, 8, 9, 10, 11, 12, 13, 14, 15, 16, 17, 18]. It is very hard to elucidate the phase diagram of the d-p model because of strong correlation between electrons. We often use simplified models such as the two-dimensional single-band Hubbard model[19, 20, 21, 22, 23, 24, 25, 26, 27, 28, 29, 30, 31, 32, 33, 34, 35, 36] or ladder model[37, 38, 39, 40] to make clear the phase diagram of correlated electron systems.

A variational Monte Carlo method is a useful method to investigate electronic properties of strongly correlated electron systems where we calculate the expectation values numerically. It is necessary to improve variational wave functions to obtain reliable results for correlated electrons. We proposed wave functions by multiplying an initial wave function by $\exp(-S)$-type operators[36, 41], where S is a correlation operator with variational parameters. An optimization

process is performed in a systematic way by multiplying by the exponential-type operators repeatedly[41]. It has been shown that the ground-state energy is lowered considerably by using this type of wave functions[36].

2. Hamiltonian

The three-band model that explicitly includes oxygen p and copper d orbitals contains the parameters U_d, U_p, t_{dp}, t_{pp}, t'_d, ϵ_d and ϵ_p. Our study is within the hole picture and the Hamiltonian is written as

$$\begin{aligned} H_{dp} &= \epsilon_d \sum_{i\sigma} d^\dagger_{i\sigma} d_{i\sigma} + \epsilon_p \sum_{i\sigma} (p^\dagger_{i+\hat{x}/2\sigma} p_{i+\hat{x}/2\sigma} + p^\dagger_{i+\hat{y}/2\sigma} p_{i+\hat{y}/2\sigma}) \\ &+ t_{dp} \sum_{i\sigma} [d^\dagger_{i\sigma} (p_{i+\hat{x}/2\sigma} + p_{i+\hat{y}/2\sigma} - p_{i-\hat{x}/2\sigma} - p_{i-\hat{y}/2\sigma}) + \text{h.c.}] \\ &+ t_{pp} \sum_{i\sigma} [p^\dagger_{i+\hat{y}/2\sigma} p_{i+\hat{x}/2\sigma} - p^\dagger_{i+\hat{y}/2\sigma} p_{i-\hat{x}/2\sigma} \\ &- p^\dagger_{i-\hat{y}/2\sigma} p_{i+\hat{x}/2\sigma} + p^\dagger_{i-\hat{y}/2\sigma} p_{i-\hat{x}/2\sigma} + \text{h.c.}] \\ &+ t'_d \sum_{\langle\langle ij \rangle\rangle \sigma} \epsilon_{ij} (d^\dagger_{i\sigma} d_{j\sigma} + \text{h.c.}) + U_d \sum_i d^\dagger_{i\uparrow} d_{i\uparrow} d^\dagger_{i\downarrow} d_{i\downarrow}. \end{aligned} \tag{1}$$

$d_{i\sigma}$ and $d^\dagger_{i\sigma}$ represent the operators for the d hole. $p_{i\pm\hat{x}/2\sigma}$ and $p^\dagger_{i\pm\hat{x}/2\sigma}$ denote the operators for the p holes at the site $R_{i\pm\hat{x}/2}$, and in a similar way $p_{i\pm\hat{y}/2\sigma}$ and $p^\dagger_{i\pm\hat{y}/2\sigma}$ are defined. t_{dp} is the transfer integral between adjacent Cu and O orbitals and t_{pp} is that between nearest p orbitals. $\langle\langle ij \rangle\rangle$ denotes a next nearest-neighbor pair of copper sites. t'_d was introduced (as shown in Fig.1) to reproduce the Fermi surface[42] reported in several cuprate superconductors such as $Bi_2Sr_2CaCu_2O_{8+\delta}$[43] and $Tl_2ba_2CuO_{6+\delta}$[44]. ϵ_{ij} takes the values ± 1 according to the sign of the transfer integral between next nearest-neighbor d orbitals. U_d is the strength of the on-site Coulomb repulsion between d holes. In this paper we neglect U_p among p holes because U_p is small compared to U_d[45, 46, 47, 48, 49]. U_p is not important in the low-doping region where the p-hole correlation effect is small. The values of band parameters were estimated as, for example, $U_d = 10.5$, $U_p = 4.0$ and $U_{dp} = 1.2$ in eV[46] where U_{dp} is the nearest-neighbor Coulomb interaction between holes on adjacent Cu and O orbitals. We neglect U_{dp} because U_{dp} is small compared to U_d. We use the notation $\Delta_{dp} = \epsilon_p - \epsilon_d$. The number of sites is denoted as N, and the total number of atoms is $N_a = 3N$. The energy unit is given by t_{dp}.

The single-band Hubbard model can be regarded as a simplified version of the three-band d-p model. This model has been studied more intensively. The Hamiltonian is given by

$$H = \sum_{ij\sigma} t_{ij} c^\dagger_{i\sigma} c_{j\sigma} + U \sum_i n_{i\uparrow} n_{i\downarrow}, \tag{2}$$

where $\{t_{ij}\}$ are transfer integrals and U is the on-site Coulomb energy. The transfer integral t_{ij} for nearest-neighbor pairs $\langle ij \rangle$ is given as $t_{ij} = -t$ and that for next-nearest neighbor pair $\langle\langle ij \rangle\rangle$ is $t_{ij} = -t'$. Otherwise, t_{ij} vanishes. The number of sites is denoted as N and the number of electrons is as N_e. The energy unit is given by t. $n_{i\sigma}$ is the number operator: $n_{i\sigma} = c^\dagger_{i\sigma} c_{i\sigma}$. The second term in the Hamiltonian represents the on-site repulsive interaction between electrons.

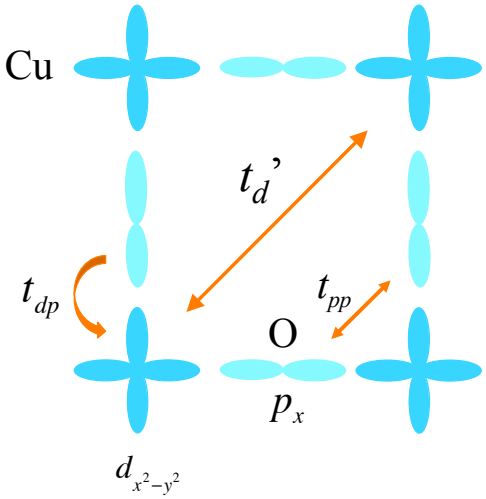

Figure 1. The transfer integral t'_d in the CuO_2 plane. t'_d is the transfer integral between next nearest-neighbor copper sites. We can also consider the transfer integral t'_{pp} between next nearest-neighbor oxygen atoms.

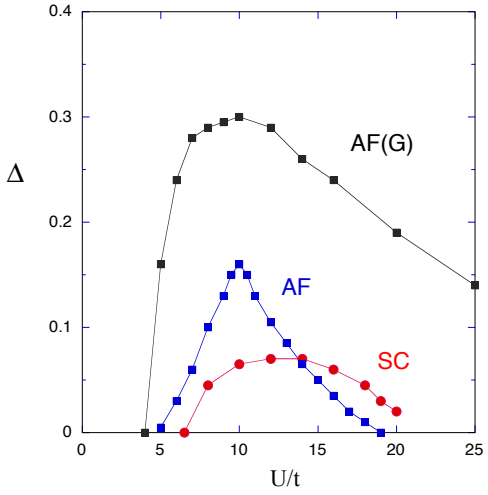

Figure 2. AF and SC order parameters as a function of U/t for the two-dimensional Hubbard model on a 10×10 lattice[36] (some data have been updated). The upper curve AF(G) indicates the result obtained by the Gutzwiller function, and those for AF and SC are obtained using ψ_λ.

3. Wave functions with strong electron correlation

The starting wave function for correlated electrons is Gutzwiller-projected wave function given by $\psi_G = P_G\psi_0$, where P_G is the Gutzwiller operator to control the double occupancy of d holes:

$$P_G = \prod_i [1-(1-g)n_{di\uparrow}n_{di\downarrow}] = \exp\left(-\alpha \sum_i n_{di\uparrow}n_{di\downarrow}\right), \tag{3}$$

where $\alpha = \ln(1/g)$. g is a variational parameter in the range from 0 to unity. $n_{di\sigma} = d^\dagger_{i\sigma}d_{i\sigma}$ is the number operator for d holes. ψ_0 is the Fermi sea where the lowest band is occupied up to the Fermi energy μ. For the d-p model, ψ_0 contains the variational parameters $\tilde{t}_{dp}$, $\tilde{t}_{pp}$, $\tilde{t}'_d$, $\tilde{\epsilon}_p - \tilde{\epsilon}_d$:

$$\psi_0 = \psi_0(\tilde{t}_{dp}, \tilde{t}_{pp}, \tilde{t}'_d, \tilde{\epsilon}_p - \tilde{\epsilon}_d). \tag{4}$$

In the non-interacting case, parameters $\tilde{t}_{dp}$, $\tilde{t}_{pp}$, $\tilde{t}'_d$ and $\tilde{\epsilon}_p - \tilde{\epsilon}_d$ coincide with those in the Hamiltonian, respectively. We fix $\tilde{t}_{dp} = t_{dp}$ as energy unit.

We consider the following wave function that is improved from the Gutzwiller wave function[36, 41, 50, 51, 52, 53, 54]:

$$\psi_\lambda = \exp(-\lambda K)\psi_G, \tag{5}$$

where λ is a variational parameter and K is the kinetic part of the Hamiltonian. The expectation values are evaluated by using the auxiliary field method[41, 55]. The kinetic part K also contains the band parameters t_{pp}, t'_d and $\epsilon_p - \epsilon_d$ as variational parameters:

$$K = K(\hat{t}_{pp}, \hat{t}'_d, \hat{\epsilon}_p - \hat{\epsilon}_d). \tag{6}$$

We take $\hat{t}_{pp} = \tilde{t}_{pp}$, $\hat{t}'_d = \tilde{t}'_d$ and $\hat{\epsilon}_p - \hat{\epsilon}_d = \tilde{\epsilon}_p - \tilde{\epsilon}_d$, for simplicity. Thus we have g, $\tilde{t}_{pp}$, $\tilde{t}'_d$, $\hat{\epsilon}_p - \hat{\epsilon}_d = \tilde{\epsilon}_p - \tilde{\epsilon}_d$, and λ as variational parameters. The expectation values for this type of

wave function are calculated by using the variational Monte Carlo method. We can evaluate the expectation value correctly within statistical errors.

The correlated superconducting (SC) state is represented by the projected-BCS wave function. This is given as

$$\psi_S = P_{N_e} P_G \psi_{BCS}, \tag{7}$$

where ψ_{BCS} indicates the BCS wave function:

$$\psi_{BCS} = \prod_{\mathbf{k}} (u_{\mathbf{k}} + v_{\mathbf{k}} \alpha^\dagger_{\mathbf{k}\uparrow} \alpha^\dagger_{-\mathbf{k}\downarrow}) |0\rangle. \tag{8}$$

$\alpha^\dagger_{\mathbf{k}\sigma}$ indicates the creation operator of the state in the lowest band with the momentum $\mathbf{k}$ which is represented by a linear combination of d and p electron operators $d^\dagger_{\mathbf{k}\sigma}$ and $p^\dagger_{\mathbf{k}\sigma}$. The BCS parameters $u_{\mathbf{k}}$ and $v_{\mathbf{k}}$ are given by the ratio $v_{bfk}/u_{\mathbf{k}} = \Delta_{\mathbf{k}}/(\xi_{\mathbf{k}} + \sqrt{\xi^2_{\mathbf{k}} + \Delta^2_{\mathbf{k}}})$ where $\xi_{\mathbf{k}}$ is the dispersion relation of the lowest band. We assume the d-wave symmetry $\Delta_{\mathbf{k}} = \Delta(\cos k_x - \cos k_y)$ and we regard Δ as the superconducting gap. Δ is a variational parameter that is optimized to give the lowest ground energy. P_{N_e} is a projection operator which extracts only the states with a fixed total hole number.

It is convenient to perform the particle-hole transformation for down-spin holes[36, 51] in multiplying by the operator $\exp(-\lambda K)$:

$$\psi_\lambda = \exp(-\lambda K) P_G \psi_{BCS} = \exp(-\lambda K) P_G \prod_{\mathbf{k}} (u_{\mathbf{k}} \beta^\dagger_{\mathbf{k}} + v_{\mathbf{k}} \alpha^\dagger_{\mathbf{k}}) |\tilde{0}\rangle, \tag{9}$$

where $\beta^\dagger_{\mathbf{k}} = \alpha_{-\mathbf{k}\downarrow}$ and $\alpha^\dagger_{\mathbf{k}} = \alpha^\dagger_{\mathbf{k}\uparrow}$. $|\tilde{0}\rangle$ denotes the vacuum for newly defined α and β particles satisfying $\alpha_{\mathbf{k}}|\tilde{0}\rangle = \beta_{\mathbf{k}}|\tilde{0}\rangle = 0$.

4. Antiferromagnetic phase and t'_d

In the two-dimensional Hubbard model, the antiferromagnetic (AF) correlation can be controlled by the Coulomb interaction U[36]. In the strongly correlated region where U is larger than the bandwidth, the antiferromagnetic correlation is suppressed and as a result superconducting state can be stable. We would expect a similar phase diagram for the d-p model. It is not, however, easy to have control of the antiferromagnetic state in the three-band d-p model. It appears that the AF state is considerably stable in the d-p model, compared to that in the single-band Hubbard model.

We show that the parameter t'_d plays an important role regarding a stability of the AF state. In Fig.3 the antiferromagnetic region is exhibited in the plane of t'_d and the level difference $\epsilon_p - \epsilon_d$ where we have 72 holes on 8×8 lattice with 192 atoms in total. There is a paramagnetic region for negative t'_d. When the level difference is small, the paramagnetic state can be stable for small $|t'_d|$.

There is a possibility of high-temperature superconductivity near the boundary where the AF correlation suppressed. We have three parameters U_d, $\epsilon_p - \epsilon_d$ and t'_d. For $t'_d = 0$, the AF phase exists as shown in Fig.4 where the doping rate is $\delta = 0.25$. AF order exists in a wide range of parameters. The strongly correlated d-wave superconducting state, however, exists when d and p level difference is small. The pure d-wave superconductivity may be realized in this region.

5. Superconducting wave function

We perform the electron-hole transformation for down-spin electrons to multiply the projected BCS function by the operator $\exp(-\lambda K)$. The electron (hole) number is not fixed as in the BCS

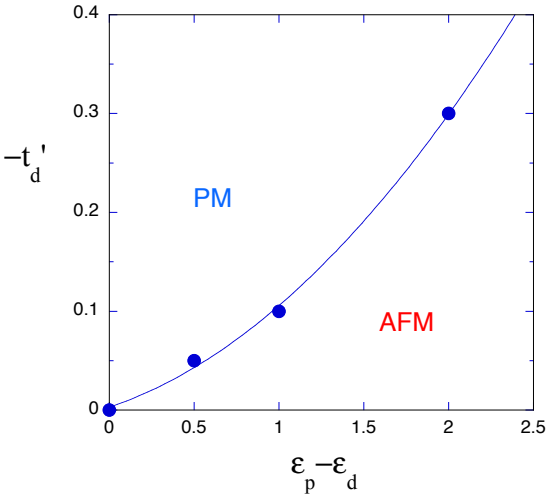

Figure 3. Antiferromagnetic region in the plane of t'_d and $\epsilon_p - \epsilon_d$ of the three-band d-p model. The energy unit is given by t_{dp}. The hole density is $\delta = 0.125$ for 72 holes on 8×8 lattice We used $t_{pp} = 0.4t_{dp}$, $U_d = 10t_{dp}$ and $U_p = 0$.

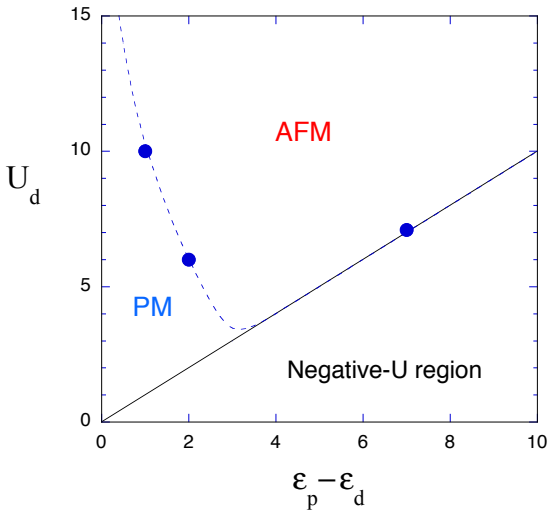

Figure 4. Antiferromagnetic region in the plane of U_d and $\epsilon_p - \epsilon_d$ in units of t_{dp} for 8×8 lattice with 76 holes. The dashed line is a guid for eyes. The band parameters are $t_{pp} = 0.4t_{dp}$,$t'_d = 0$ and $U_p = 0$.

wave function. The chemical potential is not a variational parameter since it is used to adjust the total electron number.

We show the result of calculations in Fig.5 where the total number N_h is evaluated as the expectation value by varying the chemical potential. In this result in slightly overdoped region, the optimized SC order parameter is finite indicating that the d-wave SC state is indeed realized. We expect that the SC state is stabilized in the region where $\epsilon_d - \epsilon_p$ is small and near the boundary of the AF region. There is a possibility of high-temperature superconductivity in this region.

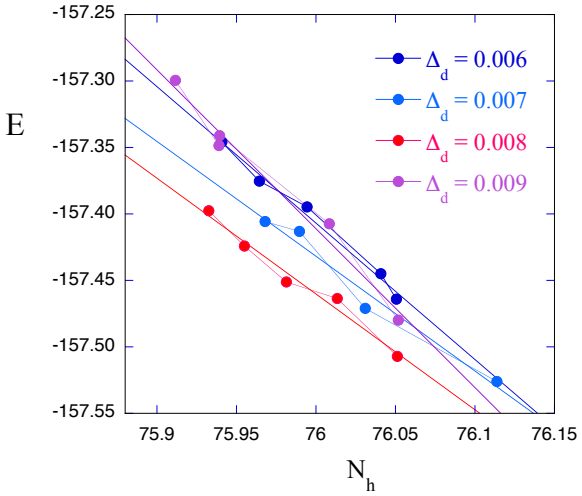

Figure 5. Total energy as a function of hole number N_h on 8×8 lattice. We set $U_d = 10$, $t_{pp} = 0$, $t'_d = 0$, $\epsilon_d = -0.5$ and $\epsilon_p = 0$. The gap parameter $\Delta = \Delta_d = \Delta_p$ is introduced for the BCS wave function. At $N_h = 76$, the energy has a minimum at finite value of Δ.

6. Discussion and Summary

It is important to determine the phase diagram in the study of correlated electron systems. In particular, we need to clarify the stability of magnetic order in electronic models of high-

temperature superconductors. For this purpose, it is necessary to improve and optimize the wave function to include electron correlation. The exponential kinetic operator $e^{-\lambda K}$ used in our work has an effect to move electrons to get the kinetic-energy gain. This will increase the double occupancy, and the variational parameters are determined to lower the ground-state energy by balancing the kinetic energy against the Coulomb repulsive energy. We can lower the ground-state energy further by multiplying the wave function by exponential kinetic operator.

The importance of multiplying by $e^{-\lambda K}$ lies in that the AF phase narrows since AF correlation is suppressed. In the 2D Hubbard model, the AF correlation is considerably suppressed when U is large being greater than the bandwidth where the kinetic-energy gain is dominant over the AF energy lowering. This also holds for the d-p model. By using the Gutzwiller function, the optimized value of the AF order parameter is very large and is larger than that of the superconducting order parameter more than by one order of magnitude in the d-p model. The AF order parameter is reduced and becomes of the same order as the superconducting one on the basis of our wave function. This would give a possibility of superconductivity.

We investigated the ground state of the two-dimensional d-p (three-band Hubbard) model by employing the optimization variational Monte Carlo method. We introduced long-range transfer intergrals t'_d to conquer the antiferromagnetism in the d-p model. We have shown the phase diagram in the plane of U_d and $\epsilon_p - \epsilon_d$. We expect that there also occurs a crossover between strongly correlated and weakly correlated regions by controlling the antiferromagnetic correlation in the d-p model. There is a crossover in the two-dimensional Hubbard model[36]. A large fluctuation presumably exists in the crossover region. This indicates a possibility of high-temperature superconductivity. A crossover from weakly to strongly coupled systems is universal phenomenon that exists ubiquitously in the world as in the Kondo effect[56, 57, 59, 60, 61, 62, 63].

References

[1] Bednorz J G and Müller K A 1986 *Z. Phys.* B **64** 189.
[2] Emery V J 1987 *Phys. Rev. Lett.* **58** 2794.
[3] Hirsch J E, Loh E Y, Scalapino D J and Tang S 1989 *Phys. Rev.* B **39** 243.
[4] Scalettar R T, Scalapino D J, Sugar R L, and White S R 1991 *Phys. Rev.* B **44** 770.
[5] Oguri A, Asahata T and Maekawa S 1994 *Phys. Rev.* B **49** 6880.
[6] Koikegami S and Yamada K 2000 *J. Phys. Soc. Jpn.* **69** 768.
[7] Yanagisawa T, Koike S and Yamaji K 2001 *Phys. Rev.* B **64** 184509.
[8] Koikegami S and Yanagisawa T 2001 *J. Phys. Soc. Jpn.* **70** 3499.
[9] Yanagisawa T, Koike S and Yamaji K 2003 *Phys. Rev.* B **67** 132408.
[10] Koikegami S and Yanagisawa T 2003 *Phys. Rev.* B **67** 134517.
[11] Koikegami S and Yanagisawa T 2006 *J. Phys. Soc. Jpn.* **75** 034715.
[12] Yanagisawa T, Miyazaki M and Yamaji K 2009 *J. Phys. Soc. Jpn.* **78** 013706.
[13] Weber C, Lauchi A, Mila F and Giamarchi T 2009 *Phys. Rev. Lett.* **102** 017005.
[14] Lau B, Berciu M and Sawatzky G A 2011 *Phys. Rev. Lett.* **106** 036401.
[15] Weber C, Giamarchi T and Varma C M 2014 *Phys. Rev. Lett.* **112** 117001.
[16] Avella A, Mancini F, Paolo F and Plekhanov E 2013 *Euro. Phys. J.* B **86** 265
[17] Ebrahimnejad H, Sawatzky G A and Berciu M 2016 *J. Phys. Cond. Matter* **28** 105603.
[18] Tamura S and Yokoyama H 2016 *Phys. Procedia* **81** 5.
[19] Hubbard J 1963 *Proc. Roy. Soc. London* **276** 238.
[20] Hubbard J 1963 *Proc. Roy. Soc. London* **281** 401.
[21] Gutzwiller M C 1963 *Phys. Rev. Lett.* **10** 159.
[22] Zhang S, Carlson J and Gubernatis J E 1997 *Phys. Rev.* B **55** 7464.
[23] Zhang S, Carlson J and Gubernatis J E 1997 *Phys. Rev. Lett.* **78** 4486.
[24] Yanagisawa T and Shimoi Y 1996 *Int. J. Mod. Phys.* B **10** 3383.
[25] Nakanishi T, Yamaji K and Yanagisawa T 1997 *J. Phys. Soc. Jpn.* **66** 294.
[26] Yamaji K, Yanagisawa T, Nakanishi T and Koike S 1998 *Physica* C **304** 225.
[27] Yamaji K, Yanagisawa T and Koike S 2000 *Physica* B **284-288** 415.
[28] Bulut N 2002 *Advances in Phys.* **51** 1587.
[29] Yokoyama H, Tanaka Y, Ogata M and Tsuchiura H 2004 *J. Phys. Soc. Jpn.* **73** 1119.
[30] Yokoyama H, Ogata M and Tanaka Y 2006 *J. Phys. Soc. Jpn.* **75** 114706.

[31] Aimi T and Imada M 2007 *J. Phys. Soc. Jpn.* **76** 113708.
[32] Miyazaki M, Yanagisawa T and Yamaji K 2004 *J. Phys. Soc. Jpn.* **73** 1643.
[33] Yanagisawa T 2008 *New J. Phys.* **10** 023014.
[34] Yanagisawa T 2013 *New J. Phys.* **15** 033012.
[35] Yanagisawa T, Miyazaki M and Yamaji K 2014 *J. Mod. Phys.* **4** 33.
[36] Yanagisawa T 2016 *J. Phys. Soc. Jpn.* **85** 114707.
[37] Noack R M, White S R and Scalapino D J 1995 *Europhys. Lett.* **30** 163.
[38] Yamaji K, Shimoi Y and Yanagisawa T 1994 *Physica* C **235** 2221.
[39] Yanagisawa T, Shimoi Y and Yamaji K 1995 *Phys. Rev.* B **52** R3860.
[40] Nakano T, Kuroki K and Onari S 2007 *Phys. Rev.* B **76** 014515.
[41] Yanagisawa T, Koike S and Yamaji K 1998 *J. Phys. Soc. Jpn.* **67** 3867.
[42] Yanagisawa T and Miyazaki M 2014 *Europhys. Lett.* **107** 27004.
[43] McElroy K, Simmonds R W, Hoffman J E, Lee D H, Orenstein J, Eisaki H, Uchida S and Davis J C 2003 *Nature* **422** 592.
[44] Hussey N E, Abdel-Jaead M, Carrington A, Mackenzie A P and Balicas L 2003 *Nature* **425** 814.
[45] Weber C, Haule K and Kotliar G 2008 *Phys. Rev.* B **78** 134519.
[46] M. Hybertsen S, Schluter M and Christensen N E 1989 *Phys. Rev.* B **39** 9028.
[47] Eskes H, Sawatzky G A and Feiner L F 1989 *Physica* C **160** 424.
[48] McMahan A K, Annett J F and Martin R M 1990 *Phys. Rev.* B **42** 6268.
[49] Eskes H and Sawatzky G 1991 *Phys. Rev.* B **43** 119.
[50] Otsuka H 1992 *J. Phys. Soc. Jpn.* **61** 1645.
[51] Yanagisawa T, Koike S and Yamaji K 1999 *J. Phys. Soc. Jpn.* **68** 3608.
[52] Eichenberger D and Baeriswyl D 2007 *Phys. Rev.* B **76** 180504.
[53] Baeriswyl D, Eichenberger D and Menteshashvii M 2009 *New J. Phys.* **11** 075010.
[54] Baeriswyl D 2011 *J. Supercond. Novel Magn.* **24** 1157.
[55] Yanagisawa T 2007 *Phys. Rev.* B **75** 224503.
[56] Kondo J 2012 *The Physics of Dilute Magnetic Alloys* (Cambridge University Press, Cambridge).
[57] Nagaoka Y 1965 *Phys. Rev.* **138** A1112.
[58] Yanagisawa T 2012 *J. Phys. Soc. Jpn.* **81** 094713.
[59] Yanagisawa T 2015 *J. Phys. Soc. Jpn.* **84** 074705.
[60] Solyom J 1979 *Adv. Phys.* **28** 201.
[61] Yanagisawa T 1991 *J. Phys. Soc. Jpn.* **60** 29.
[62] Yanagisawa T 2016 *Europhys. Lett.* **113** 41001.
[63] Yanagisawa T 2019 *Prog. Theor. Exp. Phys.* **2019** 023A01.